Photo-Cross-Linkable PNIPAAm Copolymers. 2. Effects of Constraint on Temperature and pH-Responsive Hydrogel Layers

Marianne E. Harmon,[†] Dirk Kuckling,*[,†,‡] and Curtis W. Frank*[,†]

Department of Chemical Engineering, Stanford University, Stanford, California 94305-5025, and Institut für Makromolekulare Chemie und Textilchemie, Technische Universität Dresden, D-01062 Dresden, Germany

Received July 1, 2002; Revised Manuscript Received October 25, 2002

ABSTRACT: Photo-cross-linkable co- and terpolymers of *N*-isopropylacrylamide, 2-(dimethylmaleimido)-*N*-ethyl-acrylamide as the photosensitive component, and 3-acryloylaminopropionic acid or *N*-(2-(dimethylamino)ethyl)acrylamide as ionizable comonomers were prepared by free radical polymerization. Aqueous solutions of the linear un-cross-linked co- and terpolymers showed lower critical solution temperature behavior. The phase transition temperature, which was detected by differential scanning calorimetry, ranged from 23.1 to 39.2 °C depending on the pH of the solution and the composition of the polymer. Surface plasmon resonance and optical waveguide spectroscopy were used to obtain information about the swelling behavior of hydrogel films of the photo-cross-linked polymers, giving a measurement of film thickness and refractive index. The transition temperatures of the cross-linked polymer gels showed similar trends to those of the corresponding linear polymers in solution, and the gels were shown to be both temperature- and pH-responsive, with the transition temperature ranging from 25.3 to 44.9 °C for films having a 200 nm dry film thickness. However, the swelling behavior of the cross-linked gels was found to vary as a function of dry film thickness, and three samples were selected for a more detailed study of how film thickness affects the transition temperature and swelling ratio of hydrogel films. Dry film thicknesses ranged from 9 nm to 2.3 μm, and the swelling behavior of the films fell into two distinct regimes separated by a critical thickness, which ranged from 280 to 500 nm. In the thin-film regime, the transition temperature of the films was independent of film thickness, but the refractive index of the films in the collapsed state decreased as film thickness decreased, indicating that these films are not able to fully collapse. In the thick-film regime, the swelling ratio of the films was independent of film thickness, but the transition temperature decreased as much as 2.6 °C as the film thickness increased. This was explained by the constraint imposed on the film by the presence of a fixed substrate, with the length scale of this constraint related to the critical thickness. In these films, the ionizable comonomers were found to have little effect on the swelling ratio, which is determined primarily by cross-linking density in the swollen state and by film thickness in the collapsed state.

Introduction

Temperature-responsive polymers and gels have gained great scientific and technological importance, and the characteristics of these materials have been studied extensively for applications such as drug delivery and separation systems.[1−5] Numerous techniques have been used to make films, membranes, and responsive surfaces from these materials,[6−11] and their application as chemomechanical actuators has also been proposed.[2] One of the most intensively studied polymers in this field is poly(*N*-isopropylacrylamide) (PNIPAAm), which exhibits a sharp phase transition in water upon heating above 32 °C.[3] It undergoes a temperature-induced collapse from an extended coil to a globular structure, a transition revealed on the macroscopic scale by a sudden decrease in the degree of swelling of PNIPAAm gels. Networks exhibiting such behavior are often called "responsive", "smart", or "intelligent" hydrogels.

The swelling behavior of responsive gels can be modeled as a balance between mixing free energy and rubber elasticity free energy,[12,13] and this theory has been extended to include gels of different shapes and anisotropic swelling in both one and two dimensions.[14] The transition temperature of neutral gels is determined by a balance between hydrophobic and hydrophilic side groups within the gel.[15−17] With the addition of ionizable comonomers, the osmotic contribution of the ionized groups must also be considered.[12,18−20] Applying stress to responsive hydrogels also affects the transition temperature, which increases with elongation[21] and decreases with compression.[22] The volume phase transition can be continuous or discontinuous, and coexistence between swollen and collapsed gel phases is also possible under certain conditions.[23,24]

Because swelling/deswelling is a diffusion-limited process, the macroscopic size of the gel plays an important role. The swelling rate is inversely proportional to the square of the characteristic dimension of the gel.[25] To reduce the response time to a usable level, it is therefore necessary to reduce the gel size dramatically. Our ultimate goal is to use these materials in microsystems (e.g., microactuators) in which the gel sizes are reduced to the micrometer range.[9,26,27] Despite recent advances in the photo-cross-linking of hydrophilic polymers, there have been few previous reports on the preparation of smart gels of this size.[28−31] To compare the kinetics of the volume phase transition and equilibrium swelling behavior of hydrogels over a wide range of length scales, the swelling ratio, defined as the ratio of the water-swollen film thickness to that in the dry state, and the transition temperature (T_c) under various conditions are usually the parameters of interest.

[†] Stanford University.
[‡] Technische Universität Dresden.
* To whom correspondence should be addressed. E-mail: dirk.kuckling@chemie.tu-dresden.de; curt@chemeng.stanford.edu.

10.1021/ma021025g CCC: $25.00
Published on Web 12/12/2002

Copolymer gels of NIPAAm and acidic or basic comonomers are known to be both pH- and temperature-sensitive.[32,33] The transition temperature shifts as a function of pH, and within this range of transition temperatures the gel will swell and collapse in response to changes in pH. Neutral NIPAAm gels are also affected by the presence of ions in solution, and a series of sodium halides have been used to show that different salt solutions with the same ionic strength can give dramatically different swelling behavior.[34] This complicates the analysis of the pH-sensitive copolymer gels because the change in pH is always accompanied by a change in the ionic species present in solution.[35] The change in pH will alter the charged state of the ionizable comonomers, but the ions in solution will also act to screen the interactions between those charges and act as structure breakers to decrease the entropic penalty of solution.[36] The Donnan osmotic pressure of these ions has been shown to affect the degree of swelling and the transition temperature[37,38] as well as the kinetics of gel swelling[35] and the gel mechanical properties.[39] Changing the pH while keeping the salt concentration constant gives an indication of how the two parameters act on the system, and the results can be used to explain trends in the transition temperature and the swelling ratio as a function of pH.[40] However, the effect of pH is inherently coupled to the extent of the screening interactions for different ions in solution, and the exact value of the transition temperature under a given set of conditions is often difficult to predict.

The transition temperature is known to be affected when linear responsive polymers are adsorbed to a solid substrate.[41] The transition temperature increases as the polymer chains become immobilized through contact with the substrate. This has been interpreted in terms of the fraction of tails, loops, and trains in the adsorbed polymer chains, where an increased transition temperature corresponds to an increased fraction of immobilized trains.[42] Cross-linked gels have been patterned on a solid substrate, and the presence of a fixed interface between the gel and substrate prevents the gel from expanding and contracting laterally.[26,43] There have also been reports of cross-linked gel films being affected by the presence of a fixed interface, with the interface limiting the degree of swelling perpendicular to the substrate.[44,45] The maximum degree of swelling is smaller than expected, but the presence of the interface also prevents the gel from fully collapsing.

The effect of ionic comonomers in bulk gels is to increase the swelling ratio of the gel and at the same time to increase the volume phase transition temperature.[12] In gel films, however, although the transition temperature increases as the concentration of an ionic comonomer is increased, the associated swelling is significantly reduced.[46] The stress generated by the anisotropic swelling of thicker gel films (200 μm to 5 mm) has been modeled and used to describe the formation of patterns on the gel surface.[47−49] The stress distribution has been used to explain the effects of film thickness and the osmotic pressure of ionizable groups in the gel. However, this approach has been limited to gel swelling and has not been applied to gels with a volume phase transition. These results clearly indicate an effect of film thickness, but we are not aware of any previous systematic study of how film thickness affects the swelling ratio and volume phase transition in thin films of cross-linked hydrogels.

Surface plasmon resonance (SPR) has been widely used to study polymers in thin films and at interfaces.[50] The constraint imposed by these geometries has been shown to affect characteristic transitions such as the lower critical solution temperature (LCST),[46,51] glass transition temperature,[52] and nematic transitions in liquid crystals.[53] For thin films, either the refractive index or the thickness of the film must be known. However, for thicker films, the same system can also be used to couple into waveguide modes, allowing the film thickness and refractive index to be determined independently.[52] SPR and optical waveguide spectroscopy (OWS) offer an opportunity to study thin films of responsive gels that are inaccessible by other techniques. For example, bulk gel is usually weighed to determine the solvent content and swelling ratio under various conditions.[54] Alternatively, the gel can be observed using a camera or microscope to determine the degree of swelling in response to different stimuli.[21,26,55] This approach is clearly limited to larger gel samples and is not applicable to the observation of thin gel films. For studies of microgel particles, light scattering has been used to study the swelling behavior of gel particles and colloidal particles coated with a thin layer of responsive gel.[44,45,56,57] However, because of their surface sensitivity and suitability for the study of thin films, we have used SPR and OWS to determine the refractive index and thickness of gel films as a function of temperature, pH, and ionic strength.

Experimental Section

Materials. *N*-Isopropylacrylamide (NIPAAm, Aldrich) was purified by recrystallization from hexane and dried in a vacuum. 2,2′-Azobis(isobutyronitrile) (AIBN) was recrystallized from methanol. Dioxane, tetrahydrofuran (THF), and diethyl ether were distilled over potassium hydroxide. All other reagents were of analytical grade.

Synthesis of 2-(Dimethylmaleimido)-*N*-ethylacrylamide (DMIAAm). The DMIAAm monomer was prepared according to the literature.[58]

Synthesis of 3-Acryloylaminopropionic Acid (AAmPA). The AAmPA monomer was prepared according to the literature.[59]

Synthesis of *N*-(2-(Dimethylamino)ethyl)acrylamide (DMAAAm). The DMAAAm monomer was prepared according to the literature.[27]

Synthesis of the Polymer. The PNIPAAm copolymers were obtained by free radical polymerization of NIPAAm, DMIAAm, and AAmPA or DMAAAm, initiated with AIBN in dioxane. The total monomer concentration was 0.55 mol/L, and the reaction was carried out at 70 °C under nitrogen for 7 h. The polymer was precipitated in diethyl ether and purified by reprecipitation from THF into diethyl ether (1/3). The copolymers are referred to as NIPAAm followed by the percentage feed composition of the DMIAAm chromophore (for example, NIPAAm5). All terpolymers used in this study have approximately 5% DMIAAm content, and the notation used for the terpolymers consists of the acidic or basic comonomer followed by the percentage feed composition of that comonomer (for example, AAmPA2). The name of each sample and its corresponding composition can be found in Table 1.

Characterization. The ^{1}H NMR spectra were recorded on a Bruker MSL 300 spectrometer (300 MHz). The solvent (acetone-d_6) was used as an internal reference. Differential scanning calorimetry (DSC) measurements were carried out with a TA Instruments DSC 2920 to determine the T_c of the polymer solutions. The DSC thermograms of the polymer solutions were recorded at a heating rate of 5 °C/min. The polymer concentration was 50 mg/mL in deionized water or the appropriate buffer, and the onset value of the transition was taken as T_c.[59]

Table 1. Composition of the Photo-Cross-Linkable NIPAAm Terpolymers

polymer	NIPAAm [mol %]	DMIAAm [mol %]	AAmPA [mol %]	DMAAAm [mol %]	M_w
NIPAAm5	95.5	4.5			186 000
AAmPA2	93.2	4.3	2.5		85 100
AAmPA5	89.8	5.3	4.9		114 000
AAmPA10	85.2	4.7	10.1		134 000
DMAAAm2	93.8	5.0		1.2	78 800
DMAAAm5	91.8	4.3		3.9	102 000
DMAAAm10	84.3	5.9		9.8	77 700

The molecular weight (M_w) and the molecular weight distribution (polydispersity M_w/M_n) of the copolymers were determined by gel-permeation chromatography with a Waters instrument equipped with UV and RI detectors and using Waters "Ultrastyragel" columns. The samples were measured at 30 °C in chloroform containing 0.1 vol % triethylamine as the mobile phase with a flow rate of 1 mL/min.

SPR Measurements. Polymer films for the SPR swelling experiments were prepared by spin-coating on an SPR substrate from a cyclohexanone solution containing different wt % polymer and 2 wt % thioxanthone sensitizer with respect to the polymer. The UV irradiation was carried out with a 75 W high-pressure Hg lamp at a wavelength $\lambda > 300$ nm for at least 60 min. The SPR substrates were LaSFN9 glass slides coated with a 50 nm gold film, which was deposited by evaporation with an Edwards 306 Autocoater. A more detailed description and schematic of the experimental setup can be found in ref 50. Here, we give only a short overview of the experimental technique.

Surface plasmons are excited using p-polarized light, in this case a He−Ne laser beam with a wavelength of 632.8 nm that is reflected off the gold-coated sample in the Kretchmann configuration. By varying the angle of incidence, reflectivity vs angle scans can be recorded. The observed minimum corresponds to the excitation of a surface plasmon; i.e., momentum and energy of the laser beam and the surface plasmon excitation are matched. The angle of excitation depends on both the thickness and refractive index of the dielectric on top of the gold film. The same setup can also be used for OWS when the dielectric film is sufficiently thick to act as a planar waveguide. In this case, additional minima are observed, each corresponding to the laser beam coupling into a waveguide mode. The resulting scans were fit to Fresnel calculations, and the different layers were represented as a simple box model. The SPR data comprise an average over the size of the laser beam spot (approximately 1 mm^2), and slight differences in film thickness and refractive index result in minima that are broader than those of the Fresnel calculations. This variability is indicated by error bars in each plot of refractive index and swelling ratio.

Swelling Experiments. The swelling behavior of the photo-cross-linked gel films was observed under a number of different conditions, varying pH, ionic strength, and temperature of the aqueous solution. DI water was from a Milli-Q system and had a resistivity of 18.2 MΩ·cm. Two buffer solutions were prepared: a 0.15 M buffer of disodium phosphate heptahydrate and citric acid was adjusted to pH 3, and a 0.15 M buffer of glycine, sodium chloride, and sodium hydroxide was adjusted to pH 10. The samples were placed in a flow-through cell that was connected to a peristaltic pump, and the temperature of the solute was controlled externally by a temperature-controlled bath. The temperature inside the cell was measured with a thermocouple and was accurate within 0.1 °C. The response time of the gels is on the order of seconds, which is much faster than the time scale of the temperature change in the flow cell, which is several minutes. The equilibration time between each angular scan was verified in the SPR kinetic mode, monitoring the reflected intensity at a fixed angle as a function of time, and ranged from 10 to 25 min. Thicker films were observed with optical microscopy from a 90° side view,[60] and this procedure has been reported previously.[26]

Scheme 1. Monomers Used for Polymer Synthesis

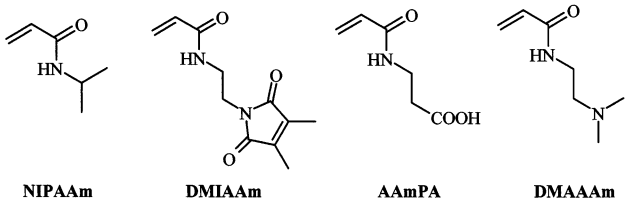

The swelling behavior of the photo-cross-linked gel films was also studied after modification of the interface between the gold substrate and the gel film. A sol−gel process was used to produce a 20 nm silica film on the gold substrate.[61] This process is compatible with SPR measurements and produces films that are stable under a wide range of pressure, pH, and temperature values. The surface energy of the gold film was also modified by a self-assembled monolayer (SAM).[62,63] Mixed SAMs of 1-hexadecanethiol (HDT) and 16-mercaptohexadecanoic acid (MHDA) on gold were prepared by submerging the gold substrates in a 1 mM solution of thiol in 200 proof ethanol under argon for 24 h. This produced surfaces with a wide range of surface energies such that the resulting contact angles were 17° for 100% MHDA, 69° for a 60:40 mixture of MHDA and HDT, and 102° for 100% HDT. Subsequent spin-coating and UV irradiation of the polymer films were carried out as described above.

Results

Temperature Response of Linear Un-Cross-Linked Polymers. Aqueous solutions of NIPAAm copolymers show LCST behavior, and because the thermal response behavior of the un-cross-linked linear polymers is retained in the networks, DSC was a convenient method to study the phase transition behavior of these polymers.[59,64] To study the influence of pH on the T_c of the photo-cross-linkable polymers, terpolymers of NIPAAm, DMIAAm, and a pH-responsive monomer, AAmPA (acidic) or DMAAAm (basic), were prepared (Scheme 1).[64] The terpolymers were synthesized with a DMIAAm feed content of 5 mol % and feed contents of AAmPA or DMAAAm of 2, 5, or 10 mol %. The composition of the polymers with various comonomer contents could be determined from ^{1}H NMR spectra recorded from polymer solutions in acetone-d_6 and by acid−base titration. The monomers selected have similar structures and should therefore have comparable reactivities, producing uniform polymers. The resulting terpolymers have compositions that are close to the feed compositions, and their physical properties are listed in Table 1.

The phase transition temperatures of the linear un-cross-linked polymers were determined from DSC measurements, and the results are shown in Figures 1 and 2. It has been suggested that LCST behavior in neutral polymers is caused by a critical hydrophobic/hydrophilic balance of the polymer side groups,[16,17] but when the polymers are ionized, it is also necessary to take into consideration the osmotic pressure of the ionizable comonomers.[15] With increasing pH, acidic copolymers become more hydrophilic as the acidic comonomers change from a noncharged to a charged state, and the same is true for basic comonomers as the pH decreases. The acidic AAmPA terpolymers (Figure 1) have a T_c that varies as a function of increasing AAmPA content, increasing at pH 10 where the comonomer is fully charged and decreasing at pH 3 where the comonomer is completely noncharged. The basic DMAAAm terpolymers (Figure 2) have an increasing T_c with increasing DMAAAm content for all pH, but the increase is more

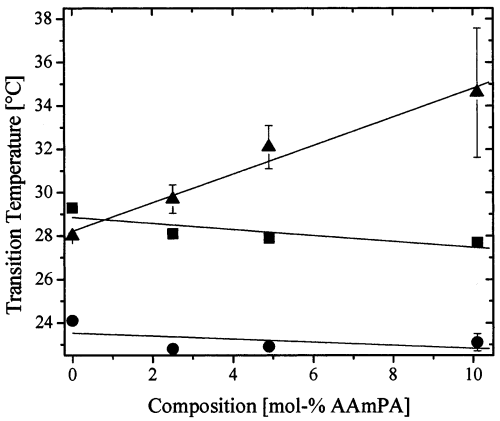

Figure 1. Phase transition temperatures for aqueous solutions of linear, un-cross-linked NIPAAm/DMIAAm/AAmPA (acidic) terpolymers as a function of composition for different pH (●, buffer pH 3; ■, DI water; ▲, buffer pH 10). Lines were drawn to guide the eye.

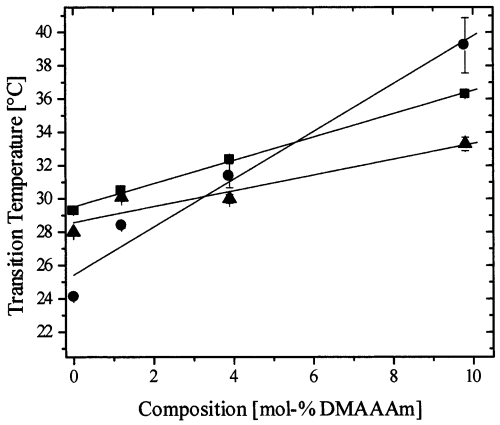

Figure 2. Phase transition temperatures for aqueous solutions of linear, un-cross-linked NIPAAm/DMIAAm/DMAAAm (basic) terpolymers as a function of composition for different pH (●, buffer pH 3; ■, DI water; ▲, buffer pH 10). Lines were drawn to guide the eye.

dramatic at pH 3 where the comonomers are fully charged. DI water has pH 5.5, but this can change slightly with the introduction of ionizable polymers. The exact pH of the samples in DI water is not known, but the results are in general intermediate to the measurements in buffers at pH 3 and pH 10.

Swelling Experiments with Photo-Cross-Linked Hydrogel Films. To fit the SPR data with a simple box model, the cross-linked gel films must consist of a thin layer with uniform thickness. Spin-coating provides very precise control over film thickness and, with a suitable solvent and spin speed, results in uniform films. Thus, a solution of the linear un-cross-linked polymer in cyclohexanone was spin-coated on the SPR substrates. The polymer concentration ranged from 0.1 to 20 wt %, and the resulting film thickness varied with the viscosity of the solution. The films were then vacuum-dried and photo-cross-linked, as shown in Scheme 2. This produced dry film thicknesses in the range of 9 nm to 2.3 μm. The refractive index of these dry films was measured by OWS on the thicker films and assumed to be constant for all film thicknesses. The dry film thickness could then be determined by either ellipsometry or SPR in air.

A combination of SPR and OWS was used to obtain information about the swelling behavior of the cross-

Scheme 2. Photo-Cross-Linking Reaction

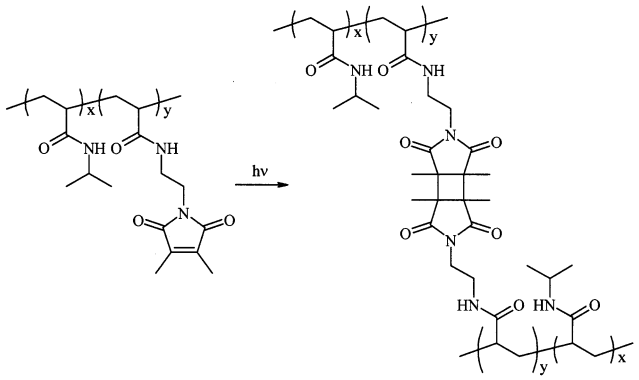

linked gel films. SPR devices measure the local average refractive index of a thin dielectric layer on top of a noble metal surface that is probed by the evanescent field of a laser beam.[50] The evanescent tail of the plasmon decays exponentially from the gold interface into the dielectric, and SPR is therefore very surface sensitive. For a constant refractive index, this can be used to measure film thickness. Conversely, if a film thickness is assumed, this method also can be used to measure the refractive index of the superposed dielectric. However, for film thicknesses greater than 300 nm, the plasmon "sees" an infinite medium, and it can be assumed that changes in the SPR minimum are caused only by changes in the refractive index. When the dielectric film is sufficiently thick to act as a planar waveguide (corresponding to a swollen film thickness of 500 nm to 1 μm for the materials in this study), the SPR setup can also be used for OWS.[50,52] For these thicker films, the position of the plasmon minimum is sensitive only to the refractive index, while the positions of the waveguide modes depend on both film thickness and refractive index. Therefore, refractive index and film thickness can be determined independently. PNIPAAm gels become opaque at temperatures above the volume phase transition, and this could contribute to scattering of the reflected laser beam. This has been observed for NIPAAm gels with grating coupling SPR,[46] but we do not expect this to be a significant problem in the Kretchmann configuration since the laser beam is reflected off the back of the gold substrate. We did not observe a significant change in the average reflected intensity or broadening of the minima in the angular scans as a function of temperature.

To study the pH sensitivity of the cross-linked gel films, 5 wt % solutions of each linear terpolymer were used. This resulted in cross-linked films with dry film thicknesses around 200 nm, which corresponds to swollen film thicknesses around 1 μm. The resulting reflectivity vs angle scans were fit to Fresnel calculations and used to solve for film thickness and refractive index as a function of temperature. The refractive index and swelling ratio, defined as the ratio of the water-swollen film thickness to that in the dry state, are shown in Figure 3 for the NIPAAm5 sample. The high refractive index at high temperatures corresponds to a collapsed and hydrophobic gel phase containing little water, while the low refractive index at low temperatures corresponds to a hydrophilic gel swollen with water.

The pH sensitivity of the gels is also apparent as the gels with an acidic comonomer, AAmPA samples shown in Figure 4, have an increased transition temperature

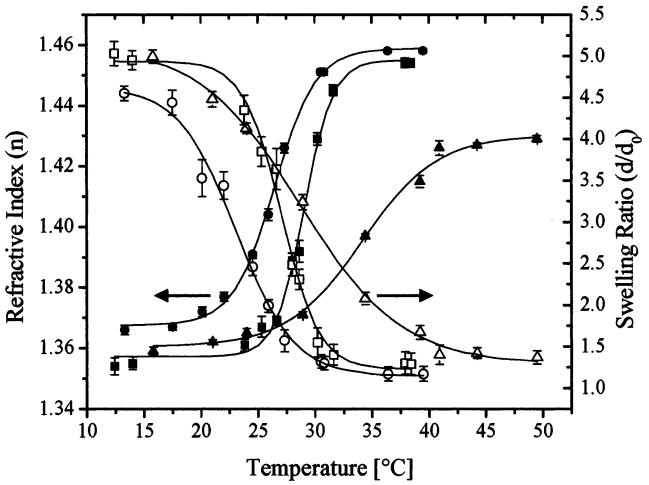

Figure 3. Refractive index (solid symbols) and swelling ratio (open symbols) of the photo-cross-linked NIPAAm5 sample are plotted as a function of temperature for different pH (●, buffer pH 3; ■, DI water; ▲, buffer pH 10). This shows the combined effect of a change in ionic strength and pH on a neutral gel. The dry film thickness of this sample is 200 nm, and the film thickness ranges from 1000 nm in the swollen state to 250 nm in the collapsed state, corresponding to the swelling ratios shown here. The Fresnel calculation to determine film thickness and refractive index is more sensitive to changes in refractive index, and the resulting error bars are consistently larger for the swelling ratio data. The difference in the steepness of the transition corresponds to the ΔT of the sigmoidal fit, as shown in Table 2.

as the pH increases. The samples with high concentrations of AAmPA have no discernible transition temperature at high pH, and sample AAmPA10 actually shows a decrease in the refractive index as a function of temperature at pH 10. As described by the Lorentz−Lorenz equation, the refractive indices of the polymer and solvent generally decrease with increased temperature due to a decrease in density,[65] and this does not correspond to a volume phase transition. The transition temperature and swelling behavior of each sample were quantified by fitting with a sigmoidal curve using the following expression:

$$n = n(\text{collapsed}) + \frac{n(\text{swollen}) - n(\text{collapsed})}{1 + \exp\left(\dfrac{T - T_c}{\Delta T_c}\right)}$$

where T_c is the inflection point of the curve, n(swollen) is the refractive index at low temperatures, n(collapsed) is the refractive index at high temperatures, and ΔT_c is a measure of the temperature range over which the transition takes place. The resulting values of T_c and ΔT_c for each sample are shown in Table 2, and the fits are shown as solid lines in each plot of refractive index vs temperature (see Figures 3−5). These data also illustrate that gels containing the basic DMAAAm comonomer have the opposite behavior to those with the acidic AAmPA comonomer, and the transition temperature increases as the pH decreases.

Effect of Varying Film Thickness. Previous measurements on similar systems have indicated that the transition temperature of gel films varies as a function of dry film thickness[60] and that the swelling ratio is limited by the presence of a solid substrate.[44−46] A more detailed analysis of the swelling behavior of these materials as a function of chromophore content has also been reported previously.[60] However, we are unaware of any previous systematic studies on the degree of swelling and the transition temperature of thin gel films as a function of film thickness. Three samples were chosen for this study: one neutral, one with acidic comonomers, and one with basic comonomers. The samples also had similar chromophore contents, resulting in films with different ionic compositions but a constant cross-linking density.

The resulting reflectivity vs angle scans were fit to Fresnel calculations, and it was clear from these data that the films could not be represented as a single uniform layer. Instead, the films were fit to a model consisting of two layers: a thinner layer near the gel−substrate interface (layer 1) and a thicker layer that represents the rest of the film (layer 2). Layer 1 has a

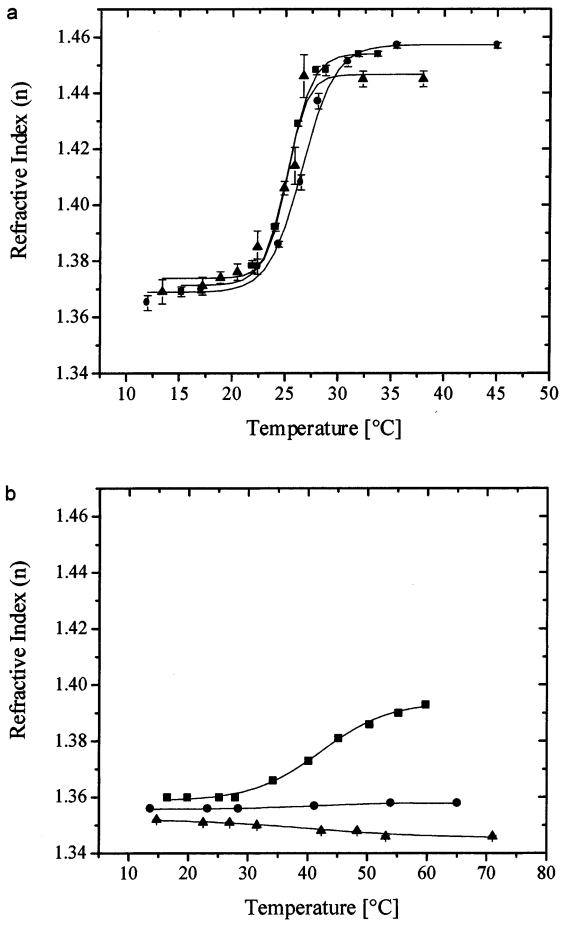

Figure 4. Refractive index of photo-cross-linked gel films at pH 3 (a) and pH 10 (b) are plotted as a function of temperature for different polymer compositions (■, AAmPA2; ●, AAmPA5; ▲, AAmPA10). The fraction of the acidic AAmPA comonomer varies for each sample, as shown in Table 1, and this illustrates the combined effects of a change in ionic strength and pH on a gel with acidic functional groups.

Table 2. Summary of Sigmoidal Fits to Swelling Data for Different pH and Ionic Strength

	buffer pH 3		DI water		buffer pH 10	
sample	T_c [°C]	ΔT	T_c [°C]	ΔT	T_c [°C]	ΔT
NIPAAM5	26.5	1.7	29.2	1.3	34.3	3.2
DMAAAm2	30.0	2.9	32.7	2.1	32.3	3.0
DMAAAm5	42.2	6.1	36.5	2.9	35.1	4.6
DMAAAm10			44.9	2.7	37.7	4.9
AAmPA2	25.4	1.1	30.0	0.5	42.2	5.7
AAmPA5	26.6	1.5	30.8	1.9		
AAmPA10	25.3	0.9	29.2	0.8		

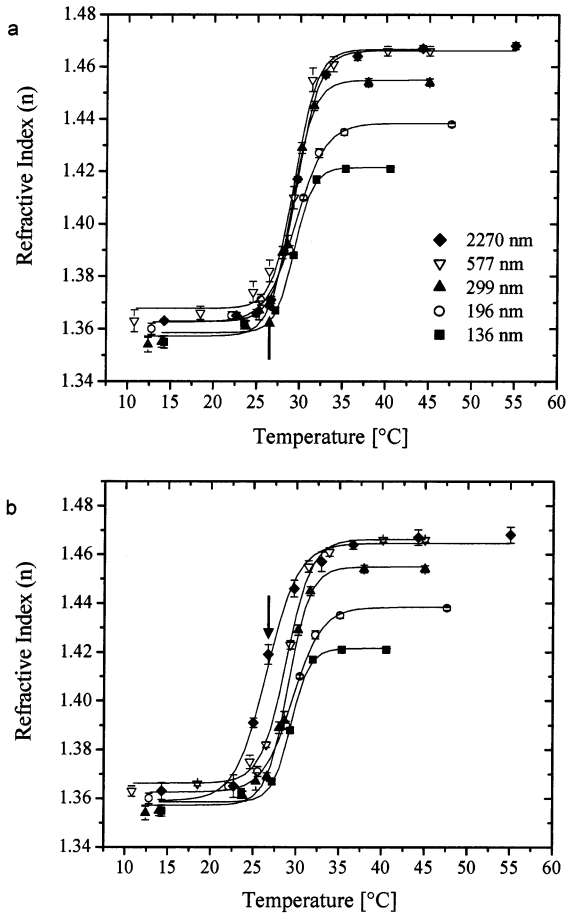

Figure 5. Refractive index of the photo-cross-linked NIPAAm5 sample is shown as a function of temperature in DI water for different film thicknesses (total thickness of dry film). The analysis of the reflectivity vs angle scans modeled the film as consisting of two layers. (a) Layer 1 is a thin layer near the gel−substrate interface and (b) layer 2 is the remaining gel film. The arrows highlight the difference between the two layers for the 2270 nm film at 26.7 °C.

refractive index lower than layer 2 for all samples, indicating that the gel at the gel−substrate interface is more swollen than the rest of the film. However, the difference is often small, less than 0.5%, with the exception of temperatures near the transition temperature, as illustrated in Figure 5. The refractive index of each layer is plotted as a function of temperature for different dry film thicknesses. For the thinner films, both layers are very similar, but for the thicker films the transition temperature of layer 2 is lower than that of layer 1. For example, as shown by the arrows in Figure 5, the 2270 nm NIPAAm5 film shows a low refractive index for layer 1 at 26.7 °C, indicating that it is fully swollen, while layer 2 has an intermediate refractive index, indicating that it is partially collapsed. Coexistence between swollen and collapsed gel phases has been demonstrated for strongly discontinuous volume phase transitions[23] and also for gels under tension.[24] The gels in this study are likely to be under stress as a result of the anisotropic swelling and the fixed substrate, and the two layers seen here are therefore consistent with previous studies of gels under constraint. The refractive index of both layers at high temperatures, corresponding to the collapsed state, also decreases as film thickness decreases.

The transition temperature and swelling ratio were measured as a function of dry film thickness for samples

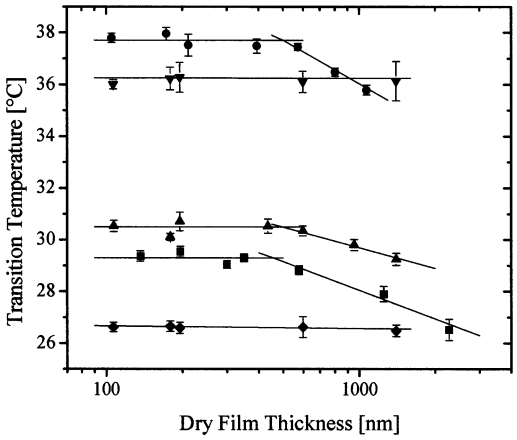

Figure 6. Summary of the transition temperature of layer 2 as a function of film thickness for neutral, acidic, and basic photo-cross-linked gels in DI water and different buffers (■, NIPAAm5 in DI water; ●, DMAAAm5 in DI water; ▲, AAmPA5 in DI water; ◆, AAmPA5 in buffer pH 3; ▼, AAmPA5 in buffer pH 10). All the data points shown are from a complete analysis of fits to Fresnel calculations. Linear fits (solid lines) were used to approximate the thickness above which the transition temperature begins to decrease. The intercepts are at 450, 500, and 500 nm for NIPAAm5, DMAAAm5, and AAmPA5, respectively.

AAmPA5 and DMAAAm5, containing 4.9% acidic AAmPA comonomer and 3.9% basic DMAAAm comonomer, respectively. Sample AAmPA5 was also observed in buffers at pH 3, 7, and 10. Although the DSC measurements show a broad transition for the linear AAmPA5 polymer at pH 10, it is clear from Figure 4b that no transition temperature can be defined for the cross-linked gel under the same conditions. However, the transition temperatures from each of the other samples can be measured, and the resulting values are plotted in Figure 6. While the transition temperature of layer 1 appears to be independent of dry film thickness (see Figure 5a), the transition temperature of layer 2 is constant for thinner films but begins to decrease above some critical film thickness. This thickness was approximated by linear fits (shown in Figure 6) to the data points above and below the apparent transition, and the resulting values were 450, 500, and 490 nm for the NIPAAm5, AAmPA5, and DMAAAm5 samples, respectively. Conversely, the data for both samples in buffer solutions show a transition temperature that is constant over the given range of film thicknesses. The Donnan equilibrium of the ions in solution can significantly affect the swelling pressure in the gel,[35,37−39] and the ions can also screen the electrostatic interactions between ionized groups in the gel.[33,35,39] Therefore, the swelling of ionized gel films in buffer is likely to be very different from the same materials in DI water. However, it is not clear from these measurements whether the transition temperature for these conditions is constant for all film thicknesses or whether the critical thickness is simply shifted beyond the range observed here. The transition temperature of sample AAmPA5 again illustrates the pH sensitivity of the gel, and the transition temperature increases as the pH increases.

The gel films discussed above have a swollen film thickness greater than 500 nm, and as a result, the thickness and refractive index of the film can be determined independently. For thinner films, it is not possible to separate the effect of the films simultaneously decreasing thickness, which will shift the plasmon resonance to lower angles, and increasing refractive

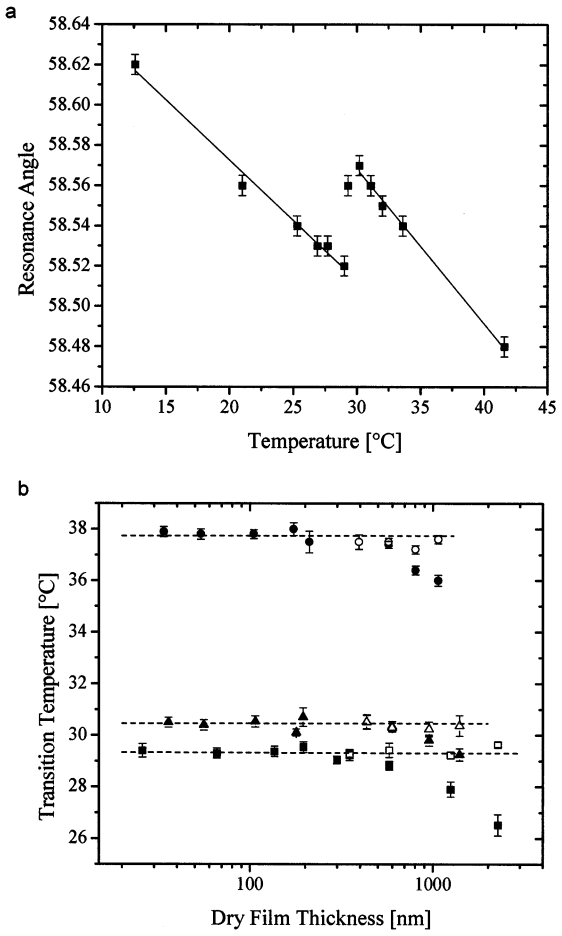

Figure 7. (a) The surface plasmon resonance angle is shown as a function of temperature for a photo-cross-linked NIPAAm5 sample with a dry film thickness of 66 nm. The discontinuity at 29.3 °C is the transition temperature of the film, and this approach is used to calculate the transition temperature for films with a dry film thickness less than 100 nm. (b) The resulting data points are shown along with those from thicknesses greater than 100 nm (■/□, NIPAAm5 in DI water; ●/○, DMAAAm5 in DI water; ▲/△, AAmPA5 in DI water), and these thicker films are modeled as having two layers. The transition temperature of the thinner films is similar to the transition temperature of layer 1 (open symbols) of the thicker films, as indicated by the dotted lines, while the transition temperature of layer 2 (solid symbols) decreases. The data points for layer 2 below 100 nm are from the analysis of θ_{SPR}, while the remaining data points are the same as in Figure 6 and are found from a complete analysis of fits to Fresnel calculations.

index, which will shift the plasmon resonance to higher angles, as the temperature increases. This is combined with the change in the refractive index of water as a function of temperature, which becomes significant as the total change in local average refractive index becomes smaller for thin films. However, by measuring the plasmon resonance angle (θ_{SPR}) as a function of temperature, it is still possible to determine a transition temperature from these data.[66] The combined effect of the above factors is to gradually shift the resonance angle to lower angles with increasing temperature, but at the transition temperature there is a distinct discontinuity in these data, corresponding to the change in the gel film (see Figure 7a). This approach was used to obtain additional values for the transition temperatures of films with a dry thickness spanning 2 orders of magnitude, and these results are shown in Figure 7b. For thicker films, the transition temperature of layer 1

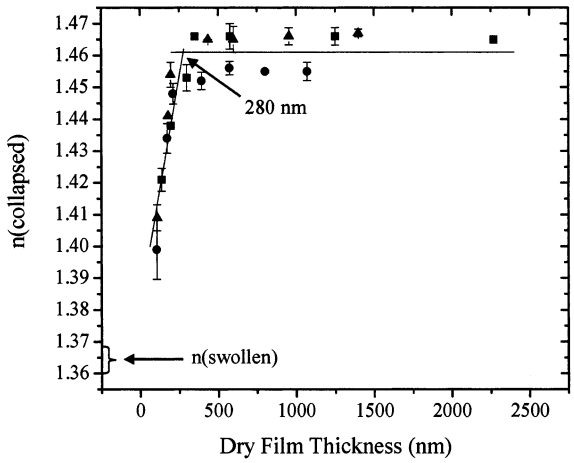

Figure 8. Summary of measurements in DI water, showing the refractive index of the photo-cross-linked gel at high temperatures as a function of dry film thickness (■, NIPAAm5; ●, DMAAAm5; ▲, AAmPA5). The refractive index is constant for thicker films and then decreases as a function of film thickness for thinner films, approaching the value of the refractive index in the swollen state. There is some variation in *n*(swollen) as a function of ionic composition, and this range is indicated by the arrow. This demonstrates that the films below 280 nm dry film thickness are unable to fully collapse at high temperatures.

is similar to that of thinner films while the transition temperature of layer 2 decreases.

As shown in Figure 5, the refractive index of the gel in its collapsed state decreases with decreasing film thickness, indicating that thin gel films are not able to fully collapse at high temperatures. The refractive index in the collapsed state is plotted as a function of dry film thickness in Figure 8 for each of the samples measured in DI water. The three samples show very similar behavior, and below some critical film thickness the refractive index decreases, corresponding to an increased swelling ratio. A thickness of 280 nm was estimated by linear fits to the data points above and below the apparent transition, as shown in Figure 8. The extrapolation of this behavior to even thinner films would suggest that at some point the gel would be completely unable to collapse, but it is not clear whether this extrapolation is meaningful.

The swelling ratio and refractive index of the cross-linked gel films in the swollen state have been shown to vary with chromophore content,[60] effectively varying the cross-linking density of the gel, while the swelling ratio in the collapsed state remains constant. However, unlike bulk gels, which are swollen by the presence of ionic groups, the effect of ionizable comonomers on the swelling ratio of the gel films is significantly reduced. This has been reported previously for PNIPAAm gel films[44−46] and is seen for the materials in this study as well. The refractive index of the films in the swollen state is also not affected by film thickness, as shown in Figure 5. As a result, the swelling ratio of these films in the swollen state is a strong function of cross-linking density but is not affected by film thickness or ionic composition. Conversely, the swelling ratio of these films in the collapsed state is determined primarily by film thickness.

Substrate Modification. Earlier studies with ATR−FTIR have shown that complete conversion of the chromophore could be achieved by UV irradiation even in thicker films and bulk samples.[60] Therefore, it is

unlikely that different gradients of cross-linking density were formed as a function of film thickness. However, it is possible that the transition temperature and swelling ratio of these gel films are somehow related to the properties of the gold substrate or the gel−substrate interface. To test this possibility, we modified the substrate by the addition of a 20 nm silica layer between the gold and the gel film. The transition temperature and swelling ratio of the NIPAAm5 sample were again measured as a function of dry film thickness. The resulting measurements were in good agreement with those on a bare gold surface, confirming that the photo-cross-linking reaction is not affected by the presence of the gold surface. The surface energy of the substrate can also affect the morphology of the resulting films, and the gold surface was therefore modified with a self-assembled monolayer, producing substrates with a wide range of surface energies. Experiments with the NIPAAm5 samples were again repeated on these functionalized gold substrates, and the resulting transition temperatures and swelling ratios were within the experimental error of the measurements on plain gold substrates shown in Figures 7b and 8.

Discussion

Solutions of Un-Cross-Linked Linear Polymers. To study "smart" hydrogel layers that respond to changes in temperature and pH, photo-cross-linkable random terpolymers based on NIPAAm, DMIAAm as the chromophore, and a third compound bearing either an acidic (AAmPA) or a basic (DMAAAm) group were prepared. As shown in Figures 1 and 2, the T_c of the acidic terpolymers in DI water decreases slightly with increasing AAmPA content, whereas T_c of the basic terpolymers in DI water increases with increasing DMAAAm content. Under these conditions the polymers are slightly charged. The same trend was found when the polymers were completely noncharged, e.g., for AAmPA terpolymers at pH 3 and for DMAAAm terpolymers at pH 10. This indicates that DMAAAm is more hydrophilic than AAmPA in the noncharged state. In the charged state, for AAmPA at pH 10 and for DMAAAm at pH 3, a strong increase of T_c with increased amount of the charged monomer was observed. The increase was as high as 6.6 °C for 9.8 mol % AAmPA and 15.1 °C for 10.1 mol % DMAAAm, as compared to the NIPAAm5 sample. It is possible to obtain a response either to temperature by overstepping the transition temperature or to pH by changing the pH in a specific temperature range limited by the transition temperatures at pH 3 and pH 10. The temperature response of ionized linear polymers is a function of the osmotic pressure of the ionizable comonomers.[15−17] The larger increase for DMAAAm is therefore an indication that the basic monomer dissociates more strongly than the acidic AAmPA and has a stronger effect on osmotic pressure.

The above trends can all be explained in terms of the hydrophobic/hydrophilic balance between the different monomers and the osmotic contributions of the ionizable comonomers in their charged states as a function of pH. However, the T_c values for all samples at pH 3 are consistently lower than those in DI water and at pH 10. This offset is around 4 °C and is most likely due to small changes in the salt concentration and variations in the ionic species in solution as the pH is adjusted. The effect of different salts on the volume phase transition is more difficult to predict, as discussed in the Introduction, and the exact origin of this offset could not be determined.

Photo-Cross-Linked Hydrogel Films. The ability of these polymers to respond to both pH and temperature provides two independent parameters that can be used to control the properties of the resulting gels. This contributes to the "smart" behavior of the gel, and the exact temperature and pH of the response can be tailored to specific applications. Also, a device containing gels with different compositions can utilize both temperature and pH to trigger specific locations within this system. Several trends are evident from the data in Figures 3 and 4 along with the summary in Table 2. The transitions of the photo-cross-linked samples in DI water are sharper (ΔT_c is smaller) than the samples measured in buffer, and there is also a difference between the two buffer solutions, with higher ΔT_c values at pH 10 than at pH 3. This is similar to the behavior of ionized bulk gels where the ions in the salt solution screen the interactions within the gel and act as structure breakers to reduce the entropic penalty of solution.[34,36,40] The presence of different ions in solution also affects the Donnan equilibrium and the swelling pressure inside the gel.[35,37−39] This results in the volume phase transition, which is discontinuous in DI water, becoming continuous and broader as the ionic strength increases. However, the combined effect of a change in pH and in ionic strength for both neutral and ionized gels has less predictable behavior. For the gel films in this study, the transition is never discontinuous, but the transition does become broader as the ionic strength increases, and this effect appears to be stronger for the buffer used at pH 10 than that used at pH 3.

Another trend is the increase in the transition temperature as the polymers become more hydrophilic with the introduction of charged comonomers. Again, the acidic AAmPA comonomer becomes ionized at high pH while the basic DMAAAm comonomer becomes ionized at low pH. The resulting changes in the swelling ratio and T_c are shown in Figure 4 and Table 2. As the gel becomes more ionized, it is clear that it is not able to form a collapsed and hydrophobic phase at high temperatures. Samples AAmPA5 and AAmPA10 are swollen and hydrophilic for all temperatures at pH 10, while sample DMAAAm10 shows a very small change in refractive index in response to temperature at pH 3, and no transition temperature was calculated for these samples. The osmotic pressure of the ions is effectively swelling the gel, and above some ionic comonomer concentration this dominates the entropic penalty of solution, causing the gel to remain swollen at all temperatures. This concentration appears to be much lower for the acidic AAmPA comonomer; therefore, the addition of a small fraction of AAmPA comonomer has a stronger effect on the swelling ratio of the gel than the same fraction of basic DMAAAm. This is in contrast to the DSC measurements on the linear un-cross-linked polymers, which indicate that the basic DMAAAm side group has a stronger effect on T_c than that of the acidic AAmPA comonomer.

Film Thickness Effects. The photo-cross-linked gel films in this study are simply physisorbed to the substrate, but the resulting swelling transition has been shown to be highly anisotropic, with the lateral swelling limited to a few percent of the swelling perpendicular to the substrate.[60] This anisotropy is itself an indication that the swelling behavior of the gel film is being

constrained by the substrate, but it does not give any indication of the length scale of the constraint. Experiments on photo-cross-linkable temperature-responsive polymers with different chromophore contents have shown a variation in the transition temperature (T_c) as a function of dry film thickness.[60] Optical microscopy measurements of 10 μm films show a transition temperature that is 4−5 °C lower than measurements of 200 nm films by SPR. This observation can be explained by the modeling of the gel films as two layers, shown in Figure 5. The optical microscopy measurement is primarily of layer 2, which makes up the majority of the film. The measurements are also on very thick films where, according to the trends shown in Figure 6, the transition temperature of layer 2 is expected to be substantially lower than that of layer 1. Conversely, the SPR measurements are of thinner films where the two layers show very similar behavior and have a higher transition temperature.

The measurements in this study show SPR and OWS measurements of films up to 2.3 μm (Figures 6 and 7b). The results show the transition temperature decreasing as a function of dry film thickness above some critical thickness, which is in the range of 450−500 nm for the materials in this study. However, it is not known over what range of thicknesses the transition temperature continues to decrease. The optical microscopy measurements may give some indication of this limit since no thickness dependence is seen for films of 10 μm dry film thickness and greater.[60] Therefore, it may be assumed that the transition temperature continues to decrease until some film thickness between 2 and 10 μm. An alternative measurement technique will be necessary to observe the behavior of these films with a dry film thickness in the range of 2−10 μm, which is too thick for OWS and too thin for optical microscopy. Previous reports of ionized gel films in the range of 200 μm to 5 cm have shown that as the gel swells perpendicular to the substrate it begins to buckle, forming patterns that vary as a function of film thickness and the osmotic pressure of the counterions.[47] This type of behavior is possible for our materials as well but has not been observed for the range of film thicknesses shown here.

The thicker films in this study are modeled as having two layers: layer 1 is near the gel−substrate interface while layer 2 makes up the remaining gel film. There are two distinct regimes for the behavior of the gels as a function of thickness (see Figure 9). First, below some critical thickness, layers 1 and 2 are very similar, and in this thin-film regime, T_c appears to be independent of film thickness. However, n(collapsed) decreases as film thickness decreases for films thinner than 280 nm, as shown in Figure 8. The second regime is found for film thicknesses above 450−500 nm. Here, n(collapsed) does not appear to be a function of film thickness, and there is a significant difference in the behavior of layers 1 and 2 near T_c, as illustrated in Figure 9. Layer 2 shows a transition temperature that decreases as film thickness increases while the transition temperature of layer 1 remains constant (see Figure 7b). Also, layer 1 is consistently more swollen than layer 2, indicating that the effect of the substrate is to prevent the gel near the interface from fully collapsing, but the difference in the refractive index is small except for temperatures near T_c. Layer 1 in the thick-film regime therefore shows many of the same characteristics as films in the thin-film regime.

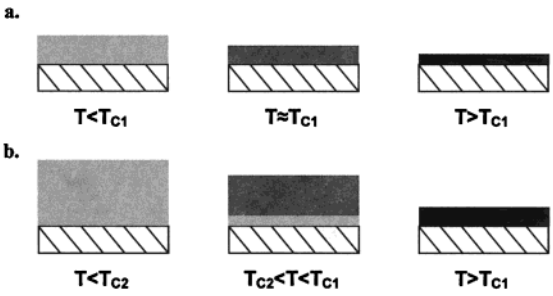

Figure 9. Summary of the photo-cross-linked gel behavior at film thicknesses in two regimes, above and below some critical film thickness. (a) Thin-film regime. Films are relatively uniform and collapse at a transition temperature T_{C1}. The extent of the collapse depends on film thickness, with thinner films not able to fully collapse at high temperatures. (b) Thick-film regime. Films have two distinct layers with layer 1, a thin region near the gel−substrate interface, having a lower refractive index than layer 2, the remaining gel. This difference is small except at temperatures near the transition temperature. Layer 2 begins to collapse at T_{C2}, which decreases as a function of film thickness, while layer 1 remains swollen at temperatures below T_{C1}.

It should be noted that the change in n(collapsed) as a function of film thickness is very similar for the three samples with similar chromophore content. The thickness below which n(collapsed) begins to decrease is also constant at 280 nm and does not appear to be affected by the presence of ionizable comonomers. This is in contrast to the transition temperature, which increases with the addition of the acidic and basic comonomers. The thickness above which the transition temperature begins to decrease also increases from 450 to 500 nm with the addition of ionizable comonomers. It is likely that the swelling behavior is actually determined by two different thicknesses, which vary with both the cross-linking density and the ionizable comonomer content of the gel films, but measurements on additional samples will be needed for a more complete understanding of these effects.

Film Uniformity. In the thick-film regime, the photo-cross-linked gel films have been modeled as having two layers, and this has been explained in terms of the distance from the substrate. However, it is important to rule out the possibility of the two layers being chemically different or having a different morphology. The lower refractive index and higher transition temperature of layer 1 are consistent with this layer having a lower cross-linking density. However, bulk polymer samples and thick films of the corresponding terpolymers can be cross-linked successfully using the same irradiation times and intensities, and the kinetics of the cross-linking reaction has been studied with ATR−FTIR.[60] Therefore, it is unlikely that the absorption of UV light by the film interferes with the cross-linking of films above a certain thickness. A gradient in cross-linking density through the film may also be caused by the depletion or segregation of the chromophores near the gel−substrate interface, but this should not reach a length scale equal to those seen in this study.

Gold has a large complex value in its refractive index, which can produce strong electromagnetic coupling between fluorescing chromophores and the metal. This leads to efficient energy transfer from the chromophore to the metal, resulting in nearly complete fluorescence quenching.[67,68] It is possible that this phenomenon could interfere with the photo-cross-linking reaction by quench-

ing the interaction between the thioxanthone sensitizer and the maleimide chromophore. This effect could cause a lower cross-linking density of the gel film closest to the gold substrate, thus producing a layer with lower refractive index at the gel−substrate interface. To further investigate this possibility, the experiments with the NIPAAm5 sample were repeated with a 20 nm layer of silica separating the gold surface and the gel film. This is a sufficiently thick barrier, larger than two Förster radii, to eliminate the coupling between the chromophores and the gold surface. However, this additional separation between the gold surface and gel film did not affect the swelling ratio or transition temperature of the resulting films. This is a good indication that the film thickness effects seen here are not related to coupling between the chromophores and the gold surface.

The surface energy of the substrate can have significant effects on the morphology of the polymer film, causing the segregation or depletion of different components at the interface[69] or the dewetting of films below a certain thickness.[70] Thus, the experiments with the NIPAAm5 sample were repeated with gold surfaces that had been functionalized with a self-assembled monolayer. The reproducibility of these experiments with a range of surface energies also eliminates the possibility of these phenomena being the result of the interfacial energy between the substrate and the gel in its hydrophobic and hydrophilic states. Having considered the possibility of interfacial energy and cross-linking density gradients causing differences in swelling ratio and transition temperatures between layers 1 and 2, we are left with the effect of the gel films being confined by a fixed substrate.

Length Scale of Constraint. There is likely to be some length scale over which the photo-cross-linked gel film "feels" the effect of the fixed substrate. The thin-film regime can be interpreted as the entire film being constrained by the substrate while the thick-film regime is characterized by only the gel near the gel−substrate interface feeling the effects of the substrate. One-dimensional swelling of ionized gels has been modeled as the gel being under compression, which increases monotonically from the substrate to the free surface.[47,49] Both compression and elongation have been shown to affect the transition temperature,[21,22] and an alternative interpretation could be that for films thicker than the critical thickness this compression is great enough to actually affect the transition temperature.

The critical thickness may be interpreted as either the length scale of constraint or the boundary between layers 1 and 2. However, this does not resolve the question of the appropriate length scale of the constraint. The critical thickness has been expressed as a dry film thickness in the range 280−500 nm. However, a film that is 500 nm in the dry state (dry atmosphere) is 620 nm in the collapsed state (DI water above T_c) and 2.5 μm in the swollen state (DI water below T_c). The temperature response and swelling behavior of the film are clearly being influenced by the presence of the fixed substrate, but it is not obvious which of these reflects the actual length scale of constraint. It is also unclear what mechanism would constrain the gel but at the same time prevent it from fully collapsing. Finally, it is possible that this length scale varies as the gel swells and collapses, altering the viscoelastic properties of the gel. Previous measurements on effects of constraint in thin films have been for polymer brushes[53] or thin films of linear polymers that are not swollen by a solvent.[52] The magnitude of the critical thicknesses reported here is greater than the length scales given in previous reports,[52,53] but the swelling phenomena in a hydrogel also generate a system with dramatically different mechanical properties. Additional measurements with a complementary technique, such as quartz crystal microbalance (QCM) or atomic force microscopy (AFM), will be necessary to resolve this issue. These techniques can be used to observe changes in the viscoelastic behavior of thin films,[71,72] which is expected to differ significantly between the dry, swollen, and collapsed states, and these results will be published in a subsequent paper.

Conclusions

Photo-cross-linkable co- and terpolymers were prepared by free radical polymerization, and the resulting linear polymers and cross-linked gel films were shown to be both pH and temperature responsive. Aqueous solutions of the un-cross-linked linear polymers showed LCST behavior, and the phase transition temperature was detected by DSC. SPR and OWS were used to obtain information about the volume phase transition of the corresponding photo-cross-linked hydrogel films and showed highly anisotropic swelling behavior. The transition temperatures of these films showed similar trends to those of the corresponding linear polymers, and this could be explained in terms of a balance between hydrophobic and hydrophilic side groups in the polymer gel and the osmotic contribution of ionizable comonomers. The swelling behavior of these films was also studied as a function of dry film thickness in the range 9 nm−2.3 μm. The swelling behavior of the films fell into two distinct regimes separated by a critical thickness, which ranged from 280 to 500 nm for all samples with a chromophore content around 5%. The transition temperature was found to vary with film thickness in the thick-film regime, and the ionizable groups were found to have little effect on the swelling ratio, which is determined primarily by cross-linking density in the swollen state and by film thickness in the collapsed state.

Acknowledgment. The DFG (Deutsche Forschungsgemeinschaft) is gratefully acknowledged for their financial support of this work within the Sonderforschungsbereich 287 "Reaktive Polymere". The work was also supported by a NSF Graduate Research Fellowship (M.E.H.) and the Center on Polymer Interfaces and Macromolecular Assemblies (CPIMA), which was sponsored by the NSF-MRSEC program under DMR 9808677. D.K. is thankful to the Max Kade foundation for a scholarship. The authors are thankful to K.-F. Arndt (TU Dresden) for help with the SLS experiments.

References and Notes

(1) Gehrke, S. H. *Adv. Polym. Sci.* **1993**, *110*, 81−144.
(2) Osada, Y.; Gong, J. P. *Adv. Mater.* **1998**, *10*, 827−837.
(3) Schild, H. G. *Prog. Polym. Sci.* **1992**, *17*, 163−249.
(4) Freitas, R. F. S.; Cussler, E. L. *Chem. Eng. Sci.* **1987**, *42*, 97−103.
(5) Dong, L.-C.; Hoffman, A. S. *J. Controlled Release* **1990**, *13*, 21−31.
(6) Yakushiji, T.; Sakai, K.; Kikuchi, A.; Aoyagi, T.; Sakurai, Y.; Okano, T. *Langmuir* **1998**, *14*, 4657−4662.
(7) Pan, Y. V.; Wesley, R. A.; Luginbuhl, R.; Denton, D. D.; Ratner, B. D. *Biomacromolecules* **2001**, *2*, 32−36.

(8) Liang, L.; Rieke, P. C.; Fryxell, G. E.; Liu, J.; Engehard, M. H.; Alford, K. L. *J. Phys. Chem. B* **2000**, *104*, 11667−11673.
(9) Ivanova, I. G.; Kuckling, D.; Adler, H.-J. P.; Wolff, T.; Arndt, K.-F. *Design. Monom. Polym.* **2000**, *3*, 447−462.
(10) Trank, S. J.; Cussler, E. L. *Chem. Eng. Sci.* **1987**, *42*, 381.
(11) Zhou, S. Q.; Wu, C. *Macromolecules* **1996**, *29*, 4998−5001.
(12) Shibayama, M.; Tanaka, T. *Adv. Polym. Sci.* **1993**, *109*, 1−62.
(13) Dusek, K.; Prins, W. *Adv. Polym. Sci.* **1969**, *6*, 1−102.
(14) Onuki, A. *Adv. Polym. Sci.* **1993**, *109*, 63−121.
(15) Taylor, L. D.; Cerankowski, L. D. *J. Polym. Sci.* **1975**, *13*, 2551−2570.
(16) Platé, N. A.; Lebedeva, T. L.; Valuev, L. I. *Polym. J.* **1999**, *31*, 21−27.
(17) Feil, H.; Bae, Y, H.; Feijen, J.; Kim, S. W. *Macromolecules* **1993**, *26*, 2496−2500.
(18) Hooper, H. H.; Baker, J. P.; Blanch, H. W.; Prausnitz, J. M. *Macromolecules* **1990**, *23*, 1096−1104.
(19) Ilavsky, M. *Macromolecules* **1982**, *15*, 782−788.
(20) Hirotsu, S. *J. Chem. Phys.* **1991**, *94*, 3949−3957.
(21) Flory, P. J. *Principles of Polymer Chemistry*; Cornell University Press: Ithaca, NY, 1953.
(22) Suzuki, A.; Kojima, S. *J. Chem. Phys.* **1994**, *101*, 10003−10007.
(23) Hirotsu, S. *Adv. Polym. Sci.* **1993**, *110*, 1−26.
(24) Suzuki, A.; Ishii, T. *J. Chem. Phys.* **1999**, *110*, 2289−2296.
(25) Tanaka, T.; Fillmore, D. J. *J. Chem. Phys.* **1979**, *70*, 1214−1218.
(26) Hoffmann, J.; Plötner, M.; Kuckling, D.; Fischer, W. J. *Sens. Actuators, Part A* **1999**, *77*, 139−144.
(27) Kuckling, D.; Adler, H.-J.; Arndt, K.-F.; Ling, L.; Habicher, W. D. *Macromol. Symp.* **1999**, *145*, 65−74.
(28) Ito, Y.; Chen, G.; Guan, Y.; Imanishi, Y. *Langmuir* **1997**, *13*, 2756−2759.
(29) Chen, G.; Imanishi, Y.; Ito, Y. *Macromolecules* **1998**, *31*, 4379−4381.
(30) Beebe, D. J.; Moore, J. S.; Bauer, J. M.; Yu, O.; Liu, R. H.; Devadoss, C.; Jo, B.-H. *Nature (London)* **2000**, *404*, 588−590.
(31) Kang, M. S.; Gupta, V. K. *J. Phys. Chem. B* **2002**, *106*, 4127−4132.
(32) Kawasaki, H.; Sasaki, S.; Maeda, H. *J. Phys. Chem. B* **1997**, *101*, 5089−5093.
(33) Hirotsu, S.; Hirokawa, Y.; Tanaka, T. *J. Chem. Phys.* **1987**, *87*, 1392−1395.
(34) Annaka, M.; Motokawa, K.; Sasaki, S.; Nakahira, T.; Kawasaki, H.; Maeda, H.; Amo, Y.; Tominaga, Y. *J. Chem. Phys.* **2000**, *113*, 5980−5985.
(35) Chou, L. Y.; Blanch, H. W.; Prausnitz, J. M. *J. Appl. Polym. Sci.* **1992**, *45*, 1411−1423.
(36) Sasaki, S.; Kawasaki, H.; Maeda, H. *Langmuir* **1999**, *15*, 4266−4269.
(37) Beltran, S.; Hooper, H. H.; Blanch, H. W.; Prausnitz, J. M. *J. Chem. Phys.* **1990**, *23*, 2061−2066.
(38) Ricka, J.; Tanaka, T. *Macromolecules* **1984**, *17*, 2916−2921.
(39) Fomenko, A.; Sedlakova, Z.; Ilavsky, M. *Polym. Bull. (Berlin)* **2001**, *47*, 367−374.
(40) Shibayama, M.; Ikkai, F.; Inamoto, S.; Nomura, S.; Han, C. C. *J. Chem. Phys.* **1996**, *105*, 4358−4365.
(41) Zhu, P. W.; Napper, D. H. *J. Colloid Interface Sci.* **1994**, *164*, 489−494.
(42) Schönhoff, M.; Larsson, A.; Welzel, P. B.; Kuckling, D. *J. Phys. Chem. B* **2002**, *106*, 7800−7808.
(43) Revzin, A.; Russell, R. J.; Yadavalli, V. K.; Koh, W.-G.; Deister, C.; Hile, D. D.; Mellott, M. B.; Pishko, M. V. *Langmuir* **2001**, *17*, 5440−5447.
(44) Kim, J.; Deike, I.; Dingenouts, N.; Norhausen, C.; Ballauff, M. *Macromol. Symp.* **1999**, *142*, 217−225.
(45) Seelenmeyer, S.; Deike, I.; Rosenfeldt, S.; Norhausen, C.; Dingenouts, N.; Ballauff, M.; Narayanan, T.; Lindner, P. *J. Chem. Phys.* **2001**, *114*, 10471−10478.
(46) Harmon, M. E.; Jakob, T. A. M.; Knoll, W.; Frank, C. W. *Macromolecules* **2002**, *35*, 5999−6004.
(47) Tanaka, T.; Sun, S.-T.; Hirokawa, Y.; Katayama, S.; Kucera, J.; Hirose, Y.; Amiya, T. *Nature (London)* **1987**, *325*, 796−798.
(48) Onuki, A. *J. Phys. Soc. Jpn.* **1988**, *57*, 1868−1871.
(49) Sekimoto, K.; Kawasaki, K. *J. Phys. Soc. Jpn.* **1987**, *56*, 2997−3000.
(50) Knoll, W. *Annu. Rev. Phys. Chem.* **1998**, *49*, 569−638.
(51) Ebihara, S.; Watanabe, T. *Kobunshi Ronbunshu* **2002**, *59*, 105−112.
(52) Prucker, O.; Christian, S.; Beck, H.; Rühe, J.; Frank, C. W.; Knoll, W. *Macromol. Chem. Phys.* **1998**, *199*, 1435−1444.
(53) Peng, B.; Johannsmann, D.; Rühe, J. *Macromolecules* **1999**, *32*, 6759−6766.
(54) Hirokawa, Y.; Tanaka, T. *J. Chem. Phys.* **1984**, *81*, 6379−6380.
(55) Suzuki, A.; Sanda, K.; Omori, Y. *J. Chem. Phys.* **1997**, *107*, 5179−5185.
(56) Wu, C.; Zhou, S. Q. *J. Polym. Sci., Part B* **1996**, *34*, 1597−1604.
(57) Hu, T. J.; Wu, C. *Phys. Rev. Lett.* **1999**, *83*, 4105−4107.
(58) Ling, L.; Habicher, W. D.; Kuckling, D.; Adler, H.-J. *Design. Monom. Polym.* **1999**, *4*, 351−358.
(59) Kuckling, D.; Adler, H.-J. P.; Arndt, K.-F.; Ling, L.; Habicher, W. D. *Macromol. Chem. Phys.* **2000**, *201*, 273−280.
(60) Kuckling, D.; Harmon, M. E.; Frank, C. W. *Macromolecules* **2002**, *35*, 6377−6383.
(61) Kambhampati, D. K.; Jakob, T. A. M.; Robertson, J. W.; Cai, M.; Pemberton, J. E.; Knoll, W. *Langmuir* **2001**, *17*, 1169−1175.
(62) Ulman, A. *An Introduction to Ultrathin Organic Films from Langmuir−Blodgett to Self-Assembly*; Academic Press: San Diego, CA, 1991.
(63) Fujihira, J.; Furugori, M.; Akiba, U.; Tani, Y. *Ultramicroscopy* **2001**, *86*, 75−83.
(64) Kuckling, D.; Adler, H.-J.; Ling, L.; Habicher, W. D.; Arndt, K.-F. *Polym. Bull. (Berlin)* **2000**, *44*, 269−276.
(65) Kleideiter, G.; Lechner, M. D.; Knoll, W. *Macromol. Chem. Phys.* **1999**, *200*, 1028−1033.
(66) Wischerhoff, E.; Zacher, T.; Laschewsky, A.; Rekai, E. D. *Angew. Chem., Int. Ed.* **2000**, *39*, 4602−4604.
(67) Enderlein, J. *Biophys. J.* **2000**, *78*, 2151−2158.
(68) Liebermann, Ts.; Knoll, W. *Colloids Surf.* **2000**, *171*, 115−130.
(69) Yang, X. M.; Peters, R. D.; Nealey, P. F.; Solak, H. H.; Cerrina, F. *Macromolecules* **2000**, *33*, 9575−9582.
(70) Fondecave, R.; Wyart, F. B. *Macromolecules* **1998**, *31*, 9305−9315.
(71) Kanekiyo, Y.; Sano, M.; Iguchi, R.; Shinkai, S. *J. Polym. Sci., Part A* **2000**, *38*, 1302−1310.
(72) Matzelle, T. R.; Ivanov, D. A.; Landwehr, D.; Heinrich, L. A.; Herkt-Bruns, C.; Reichelt, R.; Kruse, N. *J. Phys. Chem. B* **2002**, *106*, 2861−2866.

MA021025G